MNRAS **000**, 1–?? (2019) Preprint 18 July 2019 Compiled using MNRAS LATEX style file v3.0

Dark matter halo shape at $z = 0$ in the Auriga simulations: radial evolution and alignment with the stellar disk

Jesus Prada,[1⋆] Jaime E. Forero-Romero,[1] Volker Springel[2]
[1] *Departamento de Fśica, Universidad de los Andes, Cra. 1 No. 18A-10, Edificio Ip, Bogotá, Colombia.*
[2] *Heidelberg Institute for Theoretical Studies, Schloss-Wolfsbrunnenweg 35, D-69118 Heidelberg, Germany.*

Accepted XXX. Received YYY; in original form ZZZ

ABSTRACT

We present shape measurements of dark matter halos at redshift $z = 0$ in a suite of 30 cosmological simulations from the Auriga project. We compare the results in full magnetohydrodynamics against dark matter only physics. We find a strong influence of baryons in making dark matter halos rounder at all radii compared to its dark matter only counterparts. This change in triaxility is more pronounced towards the inner regions of the halo. In simulations with baryons we measure a twist in the dark matter shape as a function of radial distance; this effect is almost absent in dark matter only simulations. We quantify this twisting effect as a changing degree of alignment bewteen the halo shape with the stellar disk shape as a function of radius. An almost perfect alignment between the two components appears at $0.25R_{200} \sim 56$ kpc. We show that the twist in the radial shape evolution correlates positively with triaxility. Furthermore, at distances $\lesssim 30$ kpc, rounder and coherent dark matter distributions correlate with extended massive stellar disks and low gas densities. In a comparison against observational constraints of dark matter halo triaxiality for the Milky Way we find that 20% of halos our sample are consistent with observational results derived from the Pal 5 stream that favor $b/a \approx 1$ and $c/a > 0.77$. Including baryons is a required element to achieve this level of agreement. In contrast, all simulations (dark matter only and with baryons) are at odds with the constrains derived from the Saggitarius stream that favor $b/a \approx 0.97$ and $c/a \approx 0.44$.

Key words: galaxies: evolution — galaxies: formation — galaxies: haloes — dark matter

1 INTRODUCTION

Accurate observations and modeling of our Galaxy shape our understanding of the Universe as a whole. Explaining the Galaxy's matter composition and kinematical state is equivalent to figuring out its formation process in a cosmological context. As a first approximation, the Milky Way's (MW) morphology and separation into global kinematically coherent components, such as its disk and bulge, can be used to support the existence of a Dark Matter (DM) component to explain its dynamics around the solar neighborhood (Olling & Merrifield 2000a; Sofue et al. 2009; Catena & Ullio 2010; Bovy & Rix 2013; Iocco et al. 2015).

Improvements in the sensitivity of astronomical observations have extended this kind of modelling to outter regions of our Galaxy by measuring the stellar streams resulting from infalling globular clusters or satellite galaxies that got tidaly disrutpted by the gravitational potential of the Milky Way (Johnston 1998; Helmi & White 1999; Tremaine 1999). The interpretation of such fossil records requires the the determination of the full three-dimensional gravitational potential of the Milky Way.

The observational constraints on the gravitational potential shape can then be confronted against the expectations from different galaxy formation models in an explicit cosmological context. For instance, in the current dominant paradigm of Cold Dark Matter (CDM) dominated Universe galaxies are expected to be hosted by triaxial DM halos. To what extent the CDM expectations are born out by observations in our Galaxy? Can the MW's DM halo shape be considered typical or atypical in a cosmological context?

This ellipsoidal shape is mostly due to the anisotropical and clumpy accretion of matter influenced by environmental structures. Numerical studies how that the shape has a strong mass dependence (**?**), halos are also rounder at the

⋆ E-mail: jd.prada1760@uniandes.edu.co

outerskirts than at the inner part. Shape also evolves with cosmic time, halos get rounder as they evolve.

(Dubinski & Carlberg 1991)

Observationally some studies prefer oblate (i.e. a=b>c) configurations at small distances around $\leq$ 20 kpc (see **??**Loebman et al. 2012; Olling & Merrifield 2000b; Banerjee & Jog 2011) and more triaxial and prolate configurations on the outter distances $\geq$ 20 kpc (see Vera-Ciro & Helmi 2013; Law et al. 2009; Deg & Widrow 2013; Banerjee & Jog 2011). However, some studies are inclined towards prolate configurations even at the inner parts of the halo (see Bowden et al. 2016), and although it previously seemed that a triaxial DM halo on the outerskirts would be necessary to fully explain the characterization of the Sagittarius stream (Law et al. 2009), recent studies questioned this claim by reporting inconsistencies with narrow stellar streams Pearson et al. (2015) or finding that the relaxation of other constraints may make this claim unnecessary Ibata et al. (2013).

In simulations there is strong evidence claiming that the presence of baryons produces axisymmetrical halos. For instance, some studies have shown that the DM halo shape must be axisymmetrical to ensure the stability of a hydrodynamical disk embeded in a static DM halo. Other have studied this rounding effect by simulating the disk as rigid potential inside an N-body triaxial DM halo **?**Debattista et al. (2013); **?** finding that the halo responds to the disk by becoming less triaxial.

Rounding effect of baryons (Dubinski 1994)

The caveat of the studies mentioned above is that they do not follow baryons in the whole cosmological context. Other studies overcome this limitation by using resimulations (Abadi et al. 2010; **?**) finding that the feeback related to star formation in the disk drives the strenght of the round effect.

Abadi2010 -> well aligned countours.

Recently Chua et al. (2018) made a study in a cosmological simulation to compare the effect of including baryons. They do find, on average, rounder halo shapes once hydrodynamic effects are included, but it is uncertain the strenght of this statistical effect on galaxies similar to the MW.

(Jing & Suto 2002) report the twisting in their simulations. They also find a universal radius where the alignment of the internal region (defined as the region with 2500 times the critical density) is perfect with the shell under consideration. They blame it on high c/b and undecided vectors. but in our case c/b increases monotonically with radius, and the alignment with the disk is not monotonous. In our case this cannot be the only explanation as the triaxiliaty correlation with the twist strongly depends on the radius.

(Pedrosa et al. 2010)

All these difficulties (enough numerical resolution, explicit cosmological context, appropriate feedback physics to produce realistic MW disks) have limited the studies that want to study the rounding effect of baryons in MW-like galaxies. In this work we overcome all these limitations by analyzing the results of state-of-the-art hydrodynamical simulations of isolated halos that resemble the Milky Way. We also perform a convergence study with simulation performed at different resolution levels and explicitly compare the role of DM only vs. DM+hydro on the MW DM halo shape.

2 NUMERICAL SIMULATIONS

The Auriga project offers cosmological zoom in simulations of MW-sized dark matter halos in a ΛCDM cosmology. This simulations come in two versions: dark matter only and baryonic physics including magetohydrodynamics (MHD). A detailed description of the simulations and their disk properties can be founc in (Grand et al. 2017), here we summarize its main features.

The objects in those simulations were selected from a set of 30 isolated halos in the Evolution and Assembly of GaLaxies and their Environments (EAGLE) project (Schaye et al. 2015). These halos were randomly selected from a sample of the most isolated halos at $z = 0$ whose virial mass M_{200} was between $10^{12} M_\odot$ and $2 \times 10^{12} M_\odot$. The cosmological parameters in these simulatins correspond to $\Omega_m = 0.307$, $\Omega_b = 0.048$, $\Omega_\Lambda = 0.693$ and a dimensionless Hubble parameter $h = 0.6777$ [CITATION PLANCK 2014]

The selected halos were re-simulated at higher resultion by applying a zoom-in technique with varying physical realism using the moving-mesh AREPO code that includes gravity, ideal magnetohydrodynamics (MHD), phenomenological descriptions for star formation, chemical enrichment from supernovae and its stellar feedback. The simulation also follows the formation and evolution of black holes together with the Active Galactic Nuclei feedback (Springel 2010) [CITATIONPAKMORE].

The 30 zoom-in halos have a dark matter particle mass of $\sim 3 \times 10^5\,\mathrm{Mpc}_\odot$ while the barynic mass resolution is $\sim 5 \times 10^4\,\mathrm{Mpc}_\odot$. The softening lenght for gravitational force computation for stellar particles and high-resolution dark matter particles is fixed to be 500 h^{-1} pc in comoving coordinates up to $z = 1$, and 396 pc in physical coordinates afterwards. The gravitational softening lenght for gas cells changes with the mean cell radius but is limited to be larger than the stellar softening lenght and 1850 pc physical. This setup corresponds to `Level4` resolution. From these 30 halos, 6 of them where re-simulated at higher resolution taking into account a spatial factor of 2 in each spatial dimension, this is the `Level3` resolution. There are $\sim 4 \times 10^6$ dark matter particles within the virial radius of `Level4` halos at $z = 0$, this number increases to $\sim 3 \times 10^7$ in `Level3` simulations.

In this work all the results that we report at $z = 0$ as a function of radius and the correlations with disk properties correspond to the 30 halos in the `Level4` resolution. For the measurement on shape evolution with time we use the 6 halos in the `Level3` simulations. Finally, all halos described so far have also been simulated at the same resolutions without MHD using dark matter particles only, we refer to these halos as the DMO (Dark Matter Only) sample.

3 HALO SHAPE MEASUREMENT

The DM halo shape at a fixed radius is an estimate of either the isopotential or isodensity surfaces. Observational inference models usually estimate the isopotential contours which are probed by tracers (gas, stars), while simulations work with the isodensity contours which can be directly calculated from particle positions. Furthermore, the density contours in thin shells are very sensitive to the presence of small satelites. For this reason we measure the shape by

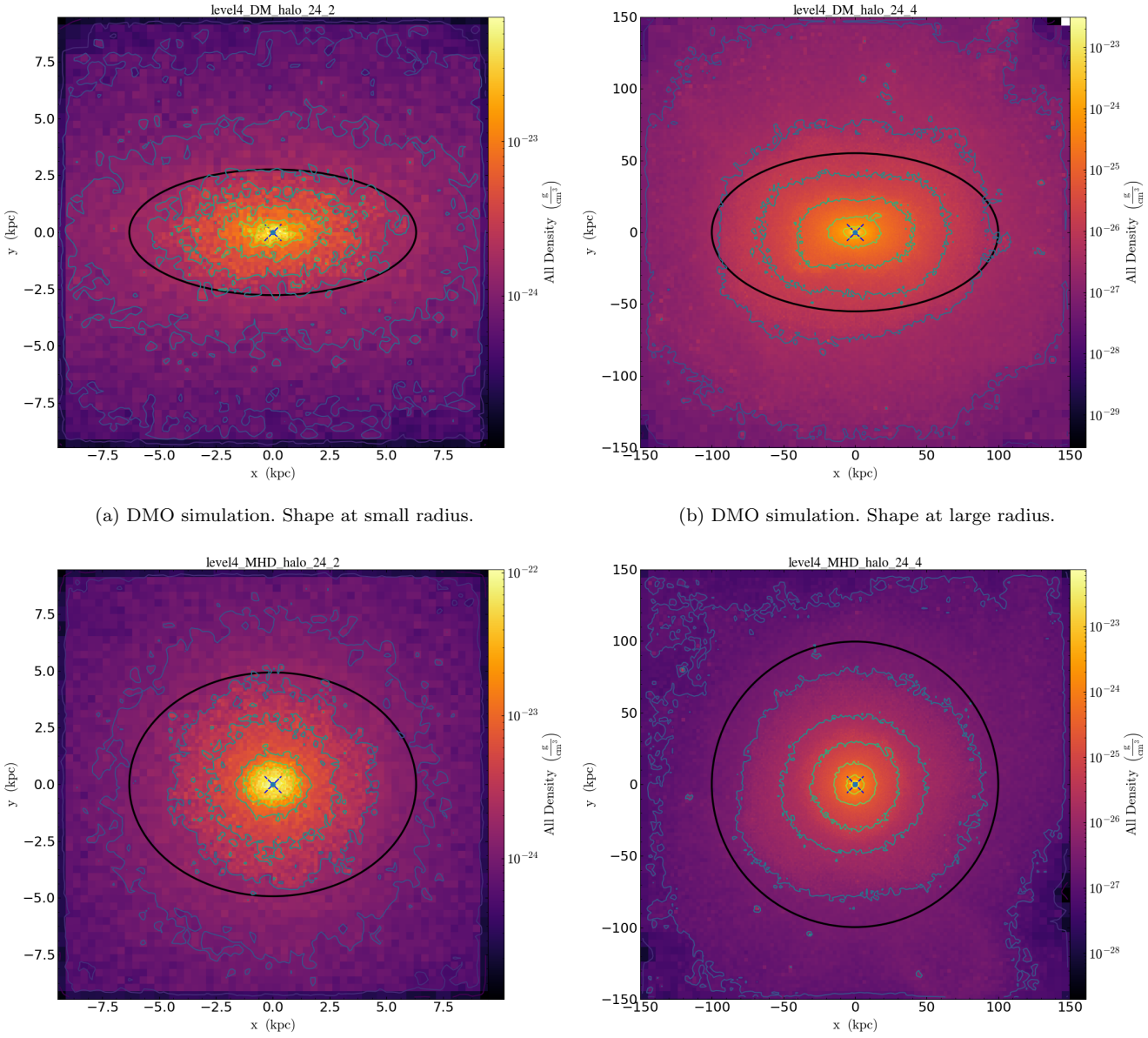

(a) DMO simulation. Shape at small radius.

(b) DMO simulation. Shape at large radius.

(c) MHD simulation. Shape at small radius.

(d) MHD simulation. Shape at large radius.

Figure 1. DM density in logarithmic scale within a slice of one tenth of the virial radius in width. The cut is perpendicular to the short axis of the inertia tensor ellipsoid. The black ellipses show the results of the fitting procedure. Upper panels correspond to DMO simulations, lower panels to MHD simulations. All cases correspond to `Level4` resolution. Left panels show data at small radii, while right panels at large radii. This halo showcases the most noticeable effect in all halos across the Auriga simulations: DM halos are rounder at all radii after baryonic physics is included.

taking volume-enclosed particles, rather than shell-enclosed. This method yields results in good agreement to the isodensity contours for radii $leq140$ kpc as explored by (Vera-Ciro et al. 2011).

In particular, we measure the shape using the reduced inertia tensor (**?**),

$$I_{ij} = \sum_k \frac{x_k^{(i)} x_k^{(j)}}{d_k^2}, \qquad (1)$$

where the particle positions are measured from the minimum of the gravitational potential in each halo and each is weighted by the k-th particle distance $d_k^2 = x_k^2 + y_k^2 + z_k^2$.

The diagonalization of this tensor yields the eigenvectors and eigenvalues that represent an ellipsoidal dark matter halo. The axis lenghts of this ellipsoid $a \geq b \geq c$ are the square root of the **I** eigenvalues and the direction of the principal axis are the corresponding eigenvectors

We start the calculations taking into account particles within a sphere of radius R and then recharacterize the triaxial parameters by taking into account particles within an ellipsoid of semi-axes $r, r/q, r/s$ and re-scaled distance $d^2 = x^2 + (y/q)^2 + (z/s)^2$, where $q = b/a$ and $s = c/a$

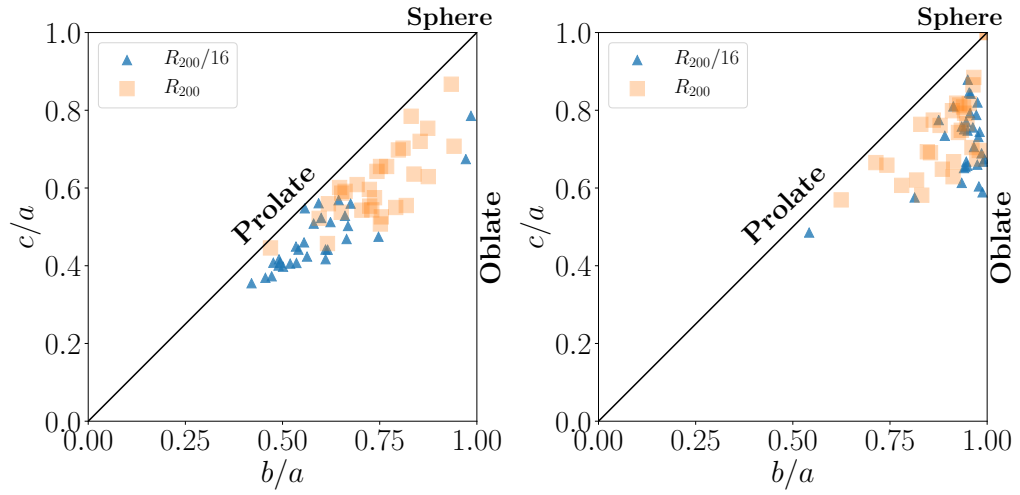

(a) DMO simulations. (b) MHD simulations.

Figure 2. Axial ratios for all halos in the simulation. Left/right panels correspond to DMO/MHD simulations, respectively. Triangles (squares) represent the measurements at $R_{200}/16$ (R_{200}) which correspond to physical distances of 14 ± 1 kpc (230 ± 15 kpc) respectively. Here we can visualize three main trends for the whole halo population. First, in DMO simulations halos are rounder in the outskirts than in the inner part. Second, halos in MHD are rounder than its DMO counterparts. Third, halos in MHD are less triaxial in the inner regions than in the outskirts.

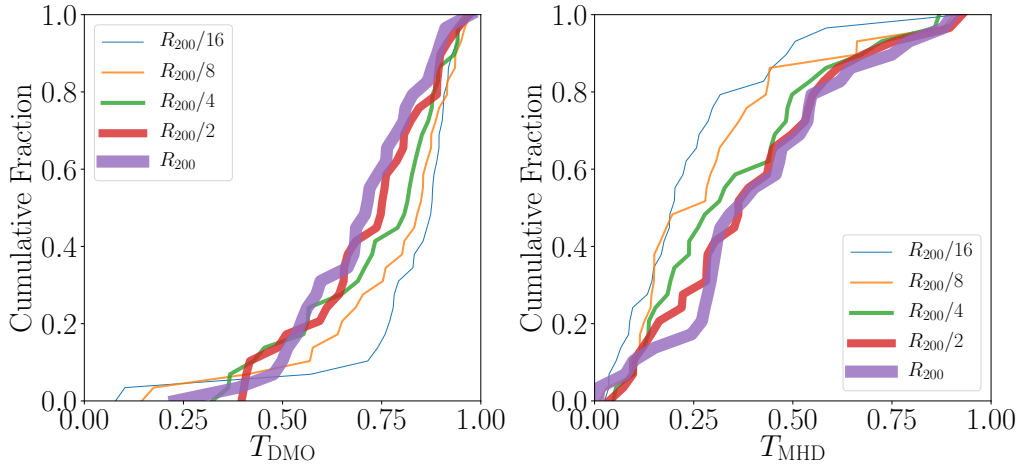

(a) DMO simulations. (b) MHD simulations.

Figure 3. Cumulative distribution for the triaxiality at five different radii. Right/left panel correspond to DMO/MHD simulations, respectively. In DMO simulations the median triaxiality at all radii is larger than 0.5; only for 20% the triaxility is smaller than 0.5. Furthermore, the triaxility increases as one moves towards the inner part of the halo. In MHD simulations the situation is reversed. The median triaxility at all radii is smaller than 0.5. Moving towards the stellar disk the triaxility decreases towards a median value of $T = 0.15$.

are the previously calculated axial ratios. We repeat this process until the average deviation of semi-axes is less than 10^{-6}. After convergence we define a unique radius R as the geometrical mean of the axial lenghts $R = (abc)^{1/3}$. We use this radial coordinate R to parameterize the spatial changes in halo shape we report in the following sections.

This is the same method used to estimate the halo shape in the DM-only Aquarius simulations (Vera-Ciro et al. 2011).

Following the convergence criterion by **?** we restrict the sampling of the ellipsoidal parameters to radii between $\sim$ 2kpc and R_{200}, where R_{200} correspond to the radius enclosing a sphere with 200 times the critical density of the Universe. On average, over the 30 halos in the `Level4` sample $R_{200} = 230 \pm 15$kpc. For `Level3` halos we go down to distances of ~ 0.2 kpc.

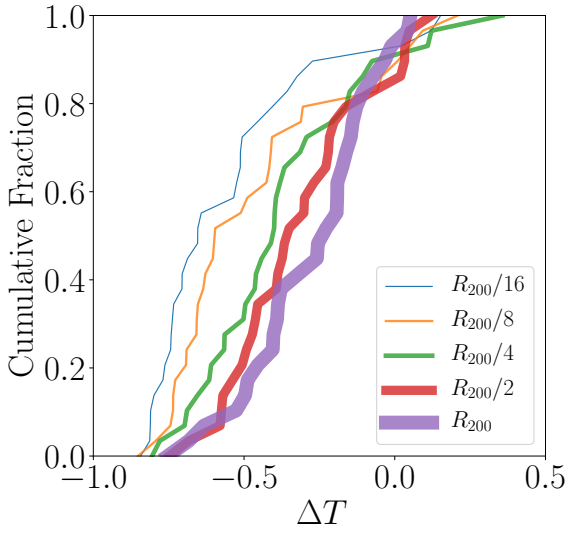

Figure 4. Cumulative distribution for the change in triaxility $\Delta T = T_{\rm MHD} - T_{\rm DMO}$ for the same radii used in Figure 3. At the virial radius all the halos become less triaxial in the MHD simulations. The change in triaxility becomes stronger in the inner regions of the dark matter halo.

4 RESULTS

4.1 Radial trends at $z = 0$

In the DMO sample we find that halos are rounder with increasing radius. The upper panels in Figure 1 illustrate this effect. The contours show a projected DM slice while the ellipsoid corresponds to the full 3D shape determination. There we see a highly ellipsoidal halo shape at radii $\sim$ 3kpc that becomes less triaxial at $\sim$ 50 kpc.

We summarize this trend in Figure 2 by plotting the results of all the 30 halos in the DMO sample. The left panel shows every halo in the c/a-b/a plane at two different radii $R_{200}/8(\sim$ 20kpc) and R_{200}. The outer part of the halo is systematically rounder than its inner region. Nevertheless the halo shape can still be considerated to be prolate at all radii. These plots confirm the results already reported in the literature (Vera-Ciro et al. 2011).

A different picture presents itself in the MHD sample. There all halos become rounder at all radii than its DMO counterpart. The lower panel in Figure 1 can be directly compared to its MHD counterpart; there we observe how at large radii the halo becomes almost spherical. The right panel in Figure 2 shows the results for the 30 halos in the MHD sample. This time the bulk of the halos can be considered oblate and close to spherical.

In Figure 3 we summarize the results at different radii using the cumulative distributions for the triaxility parameter T defined as

$$T = \frac{a^2 - b^2}{a^2 - c^2}. \qquad (2)$$

The left panel of this Figure shows that in the DMO sample the triaxility has a median larger than 0.5 at all radii, furthermore this median value increases as we move towards the inner part of the halo. The right panel shows the exact complementary picture in the MHD sampe. There the median triaxility is alwas smaller than 0.5 and this triaxility is smaller as we move closer to the galactic disk.

To quantify to what extend the global effect of decreasing triaxility in MHD simulations compared to the DMO sample holds for individual halos. We compute $\Delta T \equiv T_{\rm MHD} - T_{\rm DMO}$ the difference between the triaxility in the MHD and the DMO simulation for each individual halo. Figure shows the cumulative distribution at the same radii as in Figure .

4.2 Alignments with the stellar disk

A common assumption in observational models of the MW DM halo is that its minor axis is perfectly aligned with the stellar disk minor axis. Although it is a reasonable assumption to guarantee the stability of the galactic disk in simplified models of isolated galaxies, this might not hold in an explicit cosmological context. To examine the degree of validity of this assumption we study in this section the alignment between the eigenvectors of the inertia tensor of stellar particles within $0.1R_{200}$ ($\sim 23 \pm 2$ kpc) and the eigenvectors of the dark matter halo shape. All the measurements are done at $z = 0$.

In Figure 5 we summarize our main results regarding these alignments with the halo shape measured at five different radii. The upper row shows the alignment of the halos in the DMO simulations with the stellar disk in the MHD simulations. The main objective of this measurement is to calibrate the radial evolution of the DM halo shape. We find that the DM shape remains constant with radius.

The lower row in Figure 5 shows the alignments with the halo in the MHD simulations. This time the halo shape changes and twists at different radii. However around the radius of $0.25R_{200}$ there is an alignment almost perfect between the shapes of the stellar disk and the dark matter halo. Above and below this radius there are halos with a lower degree of alignment. Across the three different alignments we measure we verify that the strongest one is indeed the one between the two minor axis.

Statistically the strongest missalignment is found with the halo shape at a radius of $R_{200}/16 \sim (14 \pm 1)$ kpc. At this radius the mean angle and its standard deviation between the two minor axis is 18 ± 21 degrees, with one extreme case (`Au-4`) where the angle is close to 78 degrees. In contrast at $0.25R_{200}$ the angle between the two axis is 2 ± 3 degrees without any extreme outlier.

5 DISCUSSION

The first effect that we put in evidence in this paper is the effect of baryons in producing rounder DM halos. This effect has been already reported in other simulations (Debattista et al. 2008; Bryan et al. 2013; Butsky et al. 2016; Chua et al. 2019; Artale et al. 2019). The strength of the change depends on the numerical resolution, the method to resolve the hydrodynamics and the models describing star formation and stellar feedback. The key concept behind these results is that the baryon distribution influences and correlates with the dark matter halo shape. The broad tendency is that massive stellar disks correlate with spherical dark matter distributions.

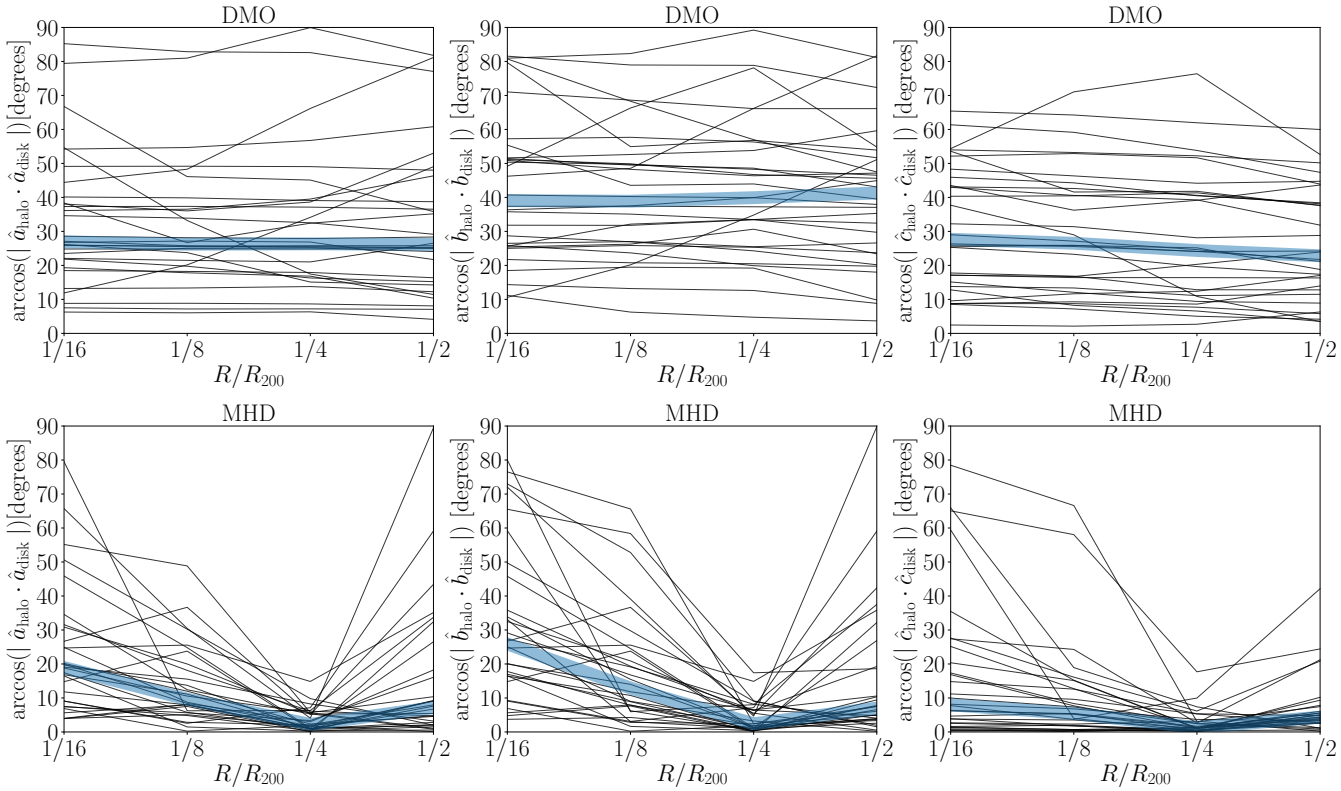

Figure 5. Angles between the principal axis of the halo shape and the principal axis of the stellar disk in the MHD simulations at four different radii $\leq 0.5R_{200}$. Thin lines correspond to each one of the thirty halos in our sample, while the thick line traces the median value. Each panel compares the alignment of the corresponding major/middle/minor axis both in the halo and the stellar disk. In the upper row the haloes come from the DMO simulation, showing that the ellipsoids describing the shape are constant as a function of radius for the most part of the sample. In the lower row the haloes come from the MHD simulation providing a self-consistent comparison with the stellar disks. In this case the dark matter shells twist in all the halos. The degree of this twisting is different in each halo. Interestingly, an almost perfect halo-disk alignment happens across the sample at an intermediate radius of $0.25R_{200}$ (56 ± 4kpc).

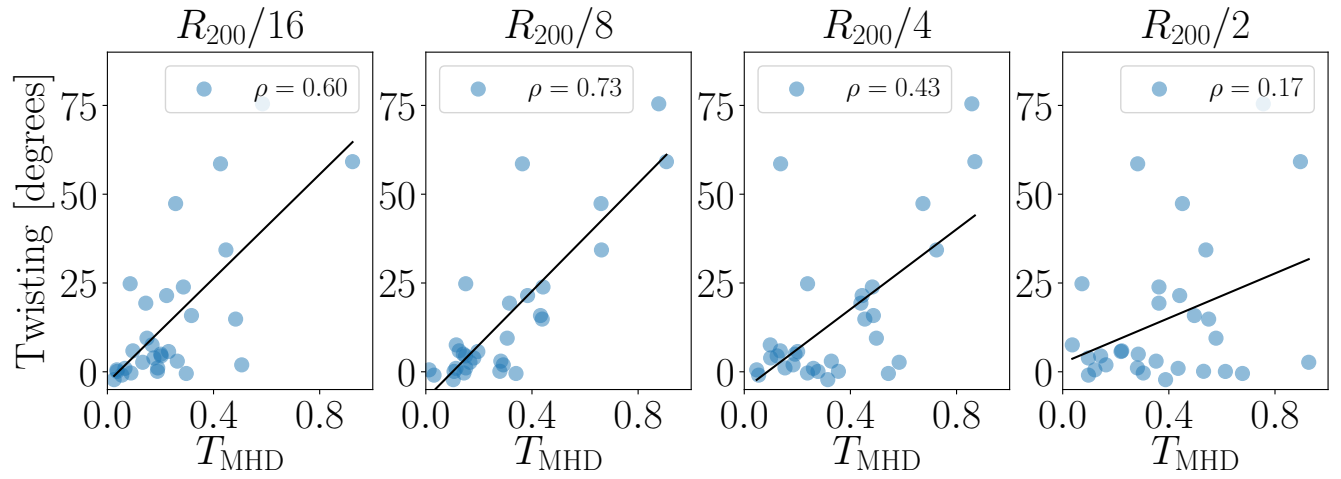

Figure 6. Changse of angle alignment of the dark matter halo and stellar disk at two different radii ($R_{200}/16$ and $0.25R_{200}$) as a function of the baryonic disk properties already explored in Figure 7. Figure 5 showed that maximum alignment occurs at $0.25R_{200}$ while in the inner regions ($R_{200}/16$) considerable missalignments occurr. at different radii and baryonic disk properties. The label with the ρ value corresponds to the SpearmanâĂŹs rank correlation coefficient.

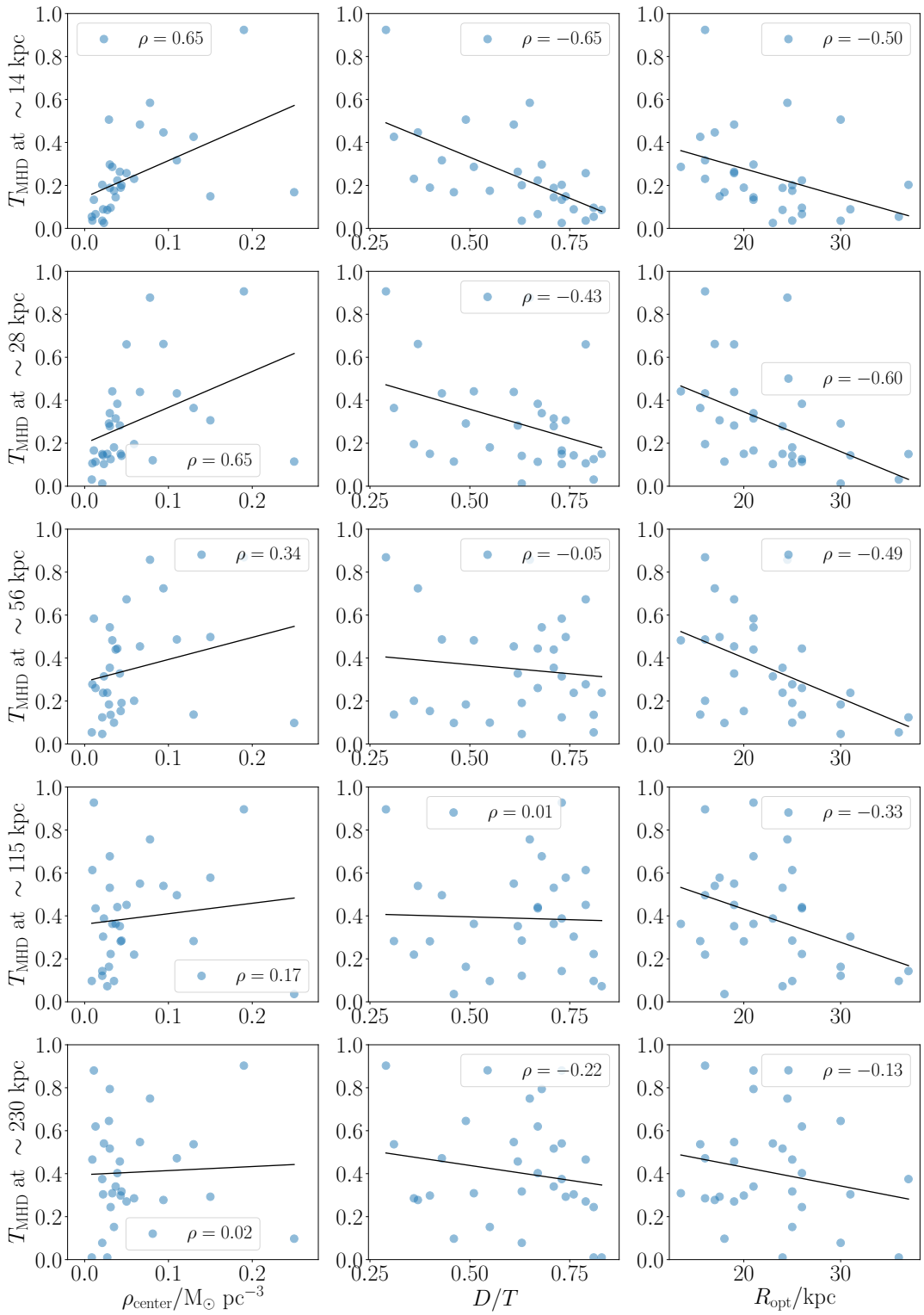

Figure 7. Correlations between the halo triaxility at different radii and baryonic disk properties. The label with the ρ value corresponds to the Spearman's rank correlation coefficient. The line is the best linear minimum squares fit. The x-axis in the first column is the gas density at the center of the galaxy with in a sphere of radius 1 kpc (Pakmor et al. 2017); the second column shows the disk to total mass ratio and the last column includes the disk optical radius defined to be the radius at which the B-band surface brightness drops below 25 mag arcsec^{-2} (Grand et al. 2017). The largest correlations are found for the two smaller radii and dilute as one approached R_{200}. Large and massive stellar disks with a low gas content are correlated with low dark matter triaxilities.

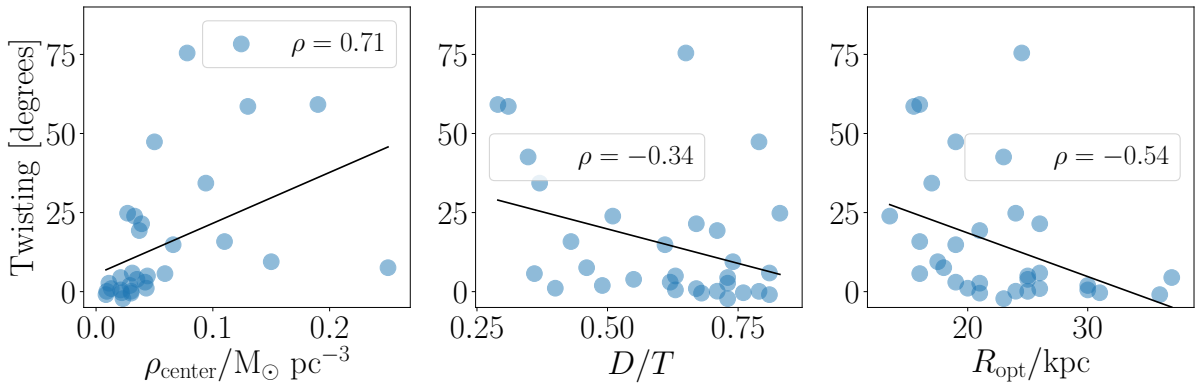

Figure 8. Changse of angle alignment of the dark matter halo and stellar disk at two different radii ($R_{200}/16$ and $0.25R_{200}$) as a function of the baryonic disk properties already explored in Figure 7. Figure 5 showed that maximum alignment occurs at $0.25R_{200}$ while in the inner regions ($R_{200}/16$) considerable missalignments occurr. at different radii and baryonic disk properties. The label with the ρ value corresponds to the SpearmanâĂŹs rank correlation coefficient.

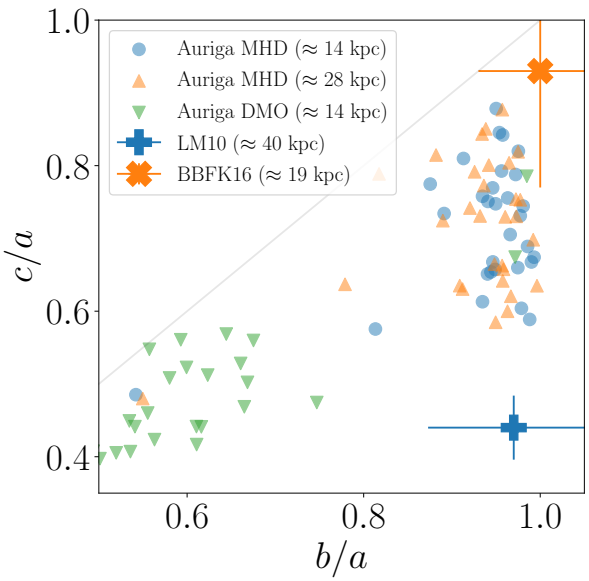

Figure 9. Comparison of our results against other simulations by Chua et al. (2019) (Illustris) and observational constraints for the dark matter halo shape in the Milky Way by Law & Majewski (2010) (LM10) and Bovy et al. (2016) (BBFK16). We report our results in the MHD simulations in such a way as to bracket the radii in the other estimates. We find that our results are broadly consistent with the Illustris simulations given the broad dispersion in both data sets. The consistency with the constraints by Bovy et al. (2016) is marginal, only 1/5 of the halos in our sample seem to be consistent within the observational reults. The result by Law & Majewski (2010) would place the Milky Way halo as an atypical object in the Λ CDM context.

In order to explore this idea in the Auriga simulations we quantify the correlation between halo shape with baronyc disk properties. Looking into the measurements already reported by Grand et al. (2017) and Pakmor et al. (2017) we find three baryonic quantities that have the strongest correlation with DM halo triaxiality: the central gas density in a sphere of radius 1kpc, the disk to total mass ratio and the optical radius.

Figure 7 summarizes the correlations of these quantities with the triaxility at five diferent radii. We use the Spearmen's rank correlation coefficient to quantify the correlation strength. This confirms our expectations. The strongest correlations are found with the halo shape measured at radii smaller than $\sim$ 28kpc, which is close to the upper limit of the disk optical radius among our simulation sample. The trend is such that halos with large triaxiality correlate with high gas density and stellar disks with low mass and small size. In turn, massive and large stellar disks with in a low density gas environment correlate with low triaxiliaty.

Using the six halos in the high resolution sample we find that the memory effect put foward by Vera-Ciro et al. (2011), that is the correlation between the historical and radial evolution of the shape, only holds for a fraction of the sample and is clearly broken for two halos in the sample. Given the small size of the sample we use to study this effect we cannot find any significant correlation with other disk properties in order to understand the shape amnesia. This effect has not been studied in detail in other simulations. We consider that understanding this effect is the first promising extension of our studies to better understand dark matter halo shape correlation with disk properties in Milky Way type galaxies. avenues to continue a deeper study on dark matter halo shape.

The second promising extension of our results deals with the shape alignment as a function of radius. In concordance with previous results in DM only simulations we find that the shells of halo shape are well aligned at different radii. The surprising result we find is that in the presences of baryons these shells twist as a function of radius. (Debattista et al. 2008) found a similar effect, but only at radii smaller than the disk radius. At radii larger than the disk radius, they find, the dark matter shells stop twisting. The twisting effect is robust across our sample of 30 halos. Also surprisingly at a radius of $0.25R_{200} \approx 56$ kpc the alignment between the stellar disk and the dark matter halo is almost perfect.

The measurements we have done in the simulations can be compared against observational results. We use the ob-

servational constraints by Law & Majewski (2010) and Bovy et al. (2016) to place our results in an observational context. Law & Majewski (2010) used observations of the long Sagittarius tidal stream to constrain the shape of the gravitational potential. Their point of depart is that previous studies that assumed an axisymetric Galactic potential were not able to fit all the available dynamic constraints for the Sagittarius stream, therefore they proposed a rigid triaxial potential, with coaxial potential ellipsoids, for the dark matter component. Their results are able to constrain the triaxility of this potential component, translating these results into a triaxiality of the density contours they report $(c/a) = 0.44$ and $(b/a) = 0.97$ at a radius of $\sim$ 40kpc. They do not report any uncertainties for these two values. Looking at their plots of their quality of fit criterion as a function of dark halo axial scales (Figure 5), we choose a conservative 10% relative uncertainty, close to the uncertainty in those parameters. The element that made the results by Law & Majewski (2010) (LM10 hereafter) surprising is that the minor axis of the halo shape is parallel, not perpendicular, to stellar disk plane.

The results by Bovy et al. (2016) (BBFK16 hereafter) have the same general approach but use instead the GD-1 (Grillmair & Dionatos 2006) and Pal 5 (Odenkirchen et al. 2009) streams to constraint the shape of the dark matter component of the galacic halo potential. They use general models with large degrees of freedom for the galactic potential in order to measure to what extent these two streams are sensitive to the triaxiality of the dark matter halo component. The DM component is written directly as a triaxial density profile with coaxial ellipsoids and the corresponding potential is found by numerical integration. They find that the width of the Pal 5 stream constraints $b/a \approx 1$ and therefore fix it to $b/a = 1$, finally they report their most stringent constrain of $c/a = 0.93 \pm 0.16$ at a radius of $\approx$ 19kpc from the galactic center.

Our Figure shows an explicit comparison in the c/a-b/a plane against the results by LM10 and BBFK16. We find 6 halos with $b/a < 0.93$ and $c/a > 0.77$ that could be considered consistent with their shape constraints by BBFK16. In contrast, none of the simulated halos is consistent with the LM10 results.

The results by LM10 would place then the dark matter halo of our Milky Way as an extreme outlier in the Λ CDM model. This extreme prolateness also correlates with the extreme triaxiality of the 11 classical satellites of the MW ($c/a \approx 0.2$, and $b/a \approx 0.9$) with an spatial distribution also oriented perpendicular to the MW plane, another highly unusual feature in the Λ CDM model (Forero-Romero & Arias 2018)

From the results presented in this work we advance the idea that the twisting shells in the density is a feature that deserves to be explored in the process of constraining shape parameters from tidal stream data. The current parameterizations of coaxial density/potential shells might be too rigid. The inclusion of a new free parameter describing this degree of twisting might relax the conflict between the observational constraints and the numerical results.

alinenaciones y twisting as a function of environment, the difference between accretting and stalled halos,

6 CONCLUSIONS

In this paper we measured the shape of thirty isolated Milky Way like dark matter haloes simulated in the Auriga project using the zoom-in technique. We also used six of these haloes that were simulated at higher resolution. The Auriga project simulated these halos with two different setups: dark matter only (DMO) simulation and full magnetohydrodynamics (MHD) includeing star formation and feedback. We used the shape measurement algorithm by Allgood et al. (2006) on the dark matter halos of these two kinds of simulations.

We find that MHD halos are rounder than DMO halos every sampled radii. MHD halos tend towards more oblate shapes (T $<$ 0.5) despite DM halos tendency towards more prolate shapes (T$>$0.5). It is also noticeable that the rounding effect of baryons is stronger at the disk regime, where the haloes are close to oblate.

This rounding effect can be explained by gravitational effect of the flattened axisymmetric galactic disk. It also explanes the weakness of this affect around $\approx$ 100kpc, where the disk potential is weaker compared to the DM halo potential.

The second part of our study on the historical shape finds that in the presence of baryons the memory effect found by (Vera-Ciro et al. 2011) does not hold for all halos in the high resolution sample.

ACKNOWLEDGEMENTS

This project has received funding from the European Union's Horizon 2020 Research and Innovation Programme under the Marie Skłodowska-Curie grant agreement No 734374.

REFERENCES

Abadi M. G., Navarro J. F., Fardal M., Babul A., Steinmetz M., 2010, MNRAS, 407, 435
Allgood B., Flores R. A., Primack J. R., Kravtsov A. V., Wechsler R. H., Faltenbacher A., Bullock J. S., 2006, MNRAS, 367, 1781
Artale M. C., Pedrosa S. E., Tissera P. B., Cataldi P., Di Cintio A., 2019, A&A, 622, A197
Banerjee A., Jog C. J., 2011, ApJ, 732, L8
Bovy J., Rix H.-W., 2013, ApJ, 779, 115
Bovy J., Bahmanyar A., Fritz T. K., Kallivayalil N., 2016, ApJ, 833, 31
Bowden A., Evans N. W., Williams A. A., 2016, MNRAS, 460, 329
Bryan S. E., Kay S. T., Duffy A. R., Schaye J., Dalla Vecchia C., Booth C. M., 2013, MNRAS, 429, 3316
Butsky I., et al., 2016, MNRAS, 462, 663
Catena R., Ullio P., 2010, J. Cosmology Astropart. Phys., 8, 004
Chua K. E., Pillepich A., Vogelsberger M., Hernquist L., 2018, preprint, (arXiv:1809.07255)
Chua K. T. E., Pillepich A., Vogelsberger M., Hernquist L., 2019, MNRAS, 484, 476
Debattista V. P., Moore B., Quinn T., Kazantzidis S., Maas R., Mayer L., Read J., Stadel J., 2008, The Astrophysical Journal, 681, 1076
Debattista V. P., Roškar R., Valluri M., Quinn T., Moore B., Wadsley J., 2013, MNRAS, 434, 2971
Deg N., Widrow L., 2013, MNRAS, 428, 912

Dubinski J., 1994, ApJ, 431, 617
Dubinski J., Carlberg R. G., 1991, ApJ, 378, 496
Forero-Romero J. E., Arias V., 2018, MNRAS, 478, 5533
Grand R. J. J., et al., 2017, Monthly Notices of the Royal Astronomical Society, 467, 179
Grillmair C. J., Dionatos O., 2006, ApJ, 641, L37
Helmi A., White S. D. M., 1999, MNRAS, 307, 495
Ibata R., Lewis G. F., Martin N. F., Bellazzini M., Correnti M., 2013, ApJ, 765, L15
Iocco F., Pato M., Bertone G., 2015, Nature Physics, 11, 245
Jing Y. P., Suto Y., 2002, ApJ, 574, 538
Johnston K. V., 1998, ApJ, 495, 297
Law D. R., Majewski S. R., 2010, The Astrophysics Journal, 714, 229
Law D. R., Majewski S. R., Johnston K. V., 2009, The Astrophysical Journal Letters, 703, L67
Loebman S. R., Ivezić Ž., Quinn T. R., Governato F., Brooks A. M., Christensen C. R., Jurić M., 2012, ApJ, 758, L23
Odenkirchen M., Grebel E. K., Kayser A., Rix H.-W., Dehnen W., 2009, AJ, 137, 3378
Olling R. P., Merrifield M. R., 2000a, MNRAS, 311, 361
Olling R. P., Merrifield M. R., 2000b, MNRAS, 311, 361
Pakmor R., et al., 2017, MNRAS, 469, 3185
Pearson S., Küpper A. H. W., Johnston K. V., Price-Whelan A. M., 2015, ApJ, 799, 28
Pedrosa S., Tissera P. B., Scannapieco C., 2010, MNRAS, 402, 776
Schaye J., et al., 2015, Monthly Notices of the Royal Astronomical Society, 446, 521
Sofue Y., Honma M., Omodaka T., 2009, PASJ, 61, 227
Springel V., 2010, Monthly Notices of the Royal Astronomical Society, 401, 791
Tremaine S., 1999, MNRAS, 307, 877
Vera-Ciro C., Helmi A., 2013, ApJ, 773, L4
Vera-Ciro C. A., Sales L. V., Helmi A., Frenk C. S., Navarro J. F., Springel V., Vogelsberger M., White S. D. M., 2011, MNRAS, 416, 1377